Int. J. Heat Mass Transfer. Vol. 28, No. 2, pp. 339–350, 1985
Printed in Great Britain

0017–9310/85 $3.00 + 0.00

Longitudinally-finned cross-flow tube banks and their heat transfer and pressure drop characteristics

E. M. SPARROW and S. S. KANG
Department of Mechanical Engineering, University of Minnesota, Minneapolis, MN 55455, U.S.A.

(*Received* 18 *April* 1984 *and in revised form* 22 *June* 1984)

Abstract—Heat transfer and pressure drop experiments were performed for cross-flow tube banks in which the individual tubes were equipped with longitudinal fins. The investigated geometrical parameters included the placement of the fins (at the front of the tube, at the rear, and at the front and rear), the fin tip shape (blunt or contoured), and the fin thickness. For each tube bank geometry, the Reynolds number was varied by nearly an order of magnitude. The results showed that a high degree of heat transfer enhancement can be obtained by finning, and the enhancements for the various tube bank geometries were compared at fixed pumping power, fixed pressure drop, and fixed mass flow. The finning-related enhancements were also compared with those attainable by the use of increased diameter unfinned tubes. Finning was found to be especially advantageous when the comparison is made at fixed pressure drop. For an array with fixed tube centers, finning permits greater additions of surface area than are possible by increases in the tube diameter.

INTRODUCTION

THIS paper explores the heat transfer and pressure drop response of an array of tubes to the presence of plate-type fins affixed to the individual tubes of the array. One of the investigated finned tube configurations is illustrated schematically in Fig. 1, which shows a typical tube of the array to which plate fins are attached both at the front and at the back. The plate fins are intended to enhance the heat transfer from the basic array. The basic array may be either a cross-flow tube bundle (i.e. with another fluid flowing inside the tubes) or a bank of pin fins. For the latter case, a configuration such as that of Fig. 1 represents the finning of fins, a heretofore little-explored concept. Throughout the paper, the word tube will be used generically, that is, it will denote either a tube or a pin fin.

Experiments were performed for three finned-tube configurations. In one, a plate fin is affixed at the front of the tube (but not at the back); this will be designated as the F configuration. In the second, a fin is affixed at the back of the tube, but not at the front (the B configuration). The third configuration, designated as F/B, is that shown in Fig. 1, where fins are attached both at the front and at the back.

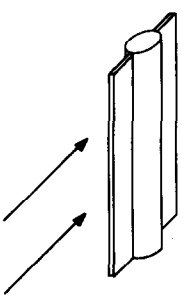

FIG. 1. Illustration of a longitudinally-finned tube situated in a cross-flow.

The effect of the shape of the fin tip on the heat transfer and pressure drop was also explored. Two fin tip geometries were employed. One is the blunt tip pictured in Fig. 1, while the other is a contoured tip whose shape will be detailed later. Another investigated parameter was the thickness of the fin, for which two values were employed.

For each finned tube configuration (defined by the fin placement (F, B or F/B), the fin tip geometry and the fin thickness), experiments were performed spanning the Reynolds number range from 1000 to 8600. The experimental results to be reported include Nusselt numbers for the individual finned tubes and dimensionless per-row pressure drops, all pertaining to the hydrodynamically developed regime. The Nusselt numbers are based both on the actual finned tube transfer surface area and also on the surface area of the unfinned tube, the latter to illustrate the heat transfer enhancement due to finning.

In addition to the experimental work, a performance analysis was made to provide perspective for the measured, fin-related heat transfer enhancements. The fin-related enhancement results from an increase in the transfer surface area. It is, therefore, relevant to inquire whether other means of increasing the transfer surface area are more or less enhancing than finning. One such alternative means is to increase the tube diameter. Comparisons of heat transfer enhancements due to finning and to diameter changes were made under the following constraints: (1) equal surface area and equal pumping power, (2) equal surface area and equal pressure drop, and (3) equal surface area and equal mass flow. In this regard, it may be noted that the surface area attainable by increasing the diameter of the unfinned tube is limited (i.e. due to contact of adjacent tubes), and that this limit is substantially lower than the surface area attainable by finning.

NOMENCLATURE

A	per-fin surface area
A'	surface area of unfinned tube, πDS
B	fins attached at back of tube
D	tube diameter
$\boldsymbol{D}$	mass diffusion coefficient
F	fins attached at front of tube
F/B	fins attached at front and back of tube
f	per-row friction factor, equation (7)
K	mass transfer coefficient based on area A, equation (3)
K'	mass transfer coefficient based on area A', equation (3)
L	fin length, Fig. 3
ΔM	per-tube mass loss
Nu	Nusselt number
PP	pumping power
Pr	Prandtl number
Δp	per-row pressure drop
Q	per-tube heat transfer rate
Re	Reynolds number, V^*D/ν
S	side of square duct; tube length
Sc	Schmidt number
Sh	Sherwood number, $KD/\boldsymbol{D}$
Sh'	Sherwood number, $K'D/\boldsymbol{D}$
S_L	longitudinal pitch
S_T	transverse pitch
t	fin thickness
t_1, t_2	fin thicknesses in Fig. 3
V^*	reference velocity, equation (6)
$\dot{w}$	per-lane mass flow rate.

Greek symbols

α	dimension ratio, S_T/D
μ	viscosity
ρ	density
ρ_{nw}	naphthalene vapor density at transfer surface
ρ_{nb}	naphthalene vapor density in bulk flow
τ	duration of data run
χ	constrained parameter.

Subscripts

o	base case (unfinned tube bank with $S_T/D = 2$)
pp	pumping power constraint.

EXPERIMENTAL

Tube bank

The unfinned tube bank which served as the basis for the experiments is illustrated schematically in Fig. 2, respectively in a top view in Fig. 2(a) and in a cross-sectional view through a typical row in Fig. 2(b). As seen in Fig. 2(a), the tubes were positioned on equilateral triangular centers. Each row consisted of six tubes, including, in alternate rows, side wall adjacent half tubes which were employed to preserve the transverse regularity of the array geometry. There was a total of 15 rows in the tube bank.

The bank was housed in a duct of square cross-section (Fig. 2(b)), with the tubes spanning the full height of the duct. Each tube was anchored to the floor of the duct by a shank integral with the lower end of the tube. The shank mated snugly with a hole in the duct floor.

Figure 2 also illustrates the dimensional nomenclature. The tube diameter is D, the transverse and longitudinal pitches are respectively denoted by S_T and S_L, and the side of the duct (equal to the length of the tubes) is S. In terms of these quantities, the investigated tube bank may be specified by the following dimension ratios:

$$S_T/D = 2,\ S_L/D = (\sqrt{3}/2)(S_T/D),\ S/D = 12. \quad (1)$$

Fins

The description of the plate fins that were affixed to the tube is facilitated by reference to Fig. 3, which shows the base-to-tip profile of the fin. The figure describes all three types of fins that were used during the course of the experiments. All three types had a common base-to-tip length L. The fins used in the first set of experiments were blunt tipped and of thickness t_1. After these

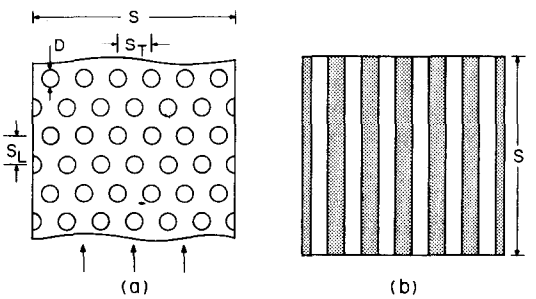

FIG. 2. Baseline unfinned tube bank: (a) top view, (b) cross-sectional view.

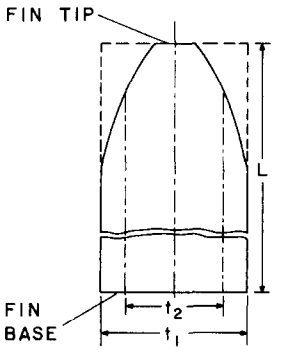

FIG. 3. Base-to-tip profile of a fin.

experiments were completed, the tip of each fin was machined with an involute gear milling cutter (24 pitch, 12 to rack) to produce the curved contours pictured in Fig. 3. Aside from the neighborhood of the tip, the thickness t_1 was maintained as before.

Experiments were then performed with the contoured-tipped fins in place, after which the fin thickness was reduced to t_2. In the machining operations employed to reduce the thickness, an identical amount of material was removed from each side of the fin in order to preserve the symmetry of the contoured tip.

Relative to the tube diameter, the dimensions of the fins are

$$L/D = 1,\ t_1/L = 0.25,\ t_2/L = 0.16. \quad (2)$$

The thicknesses t_1 and t_2 given by this equation pertain to all the finned tubes in the array except for the side wall adjacent half tubes. For the latter, half-thickness fins were employed.

With the fins in place, the tube bank takes on an appearance quite different from that of Fig. 2(a) for the unfinned tubes. To illustrate the appearance of the finned-tube arrays, representative clusters of finned tubes for each of the configurations F, B and F/B are shown in Fig. 4. The illustrated fins are the blunt-tipped, larger-thickness type. Comparison of Fig. 4 with Fig. 2(a) suggests that the presence of the fins tends to channel the flow, especially when fins are in place both at the front and the back of each tube.

Mass transfer

The heat transfer results were actually determined via mass transfer experiments performed with the naphthalene sublimation technique. As will be discussed later, the measured Sherwood numbers (dimensionless mass transfer coefficients) can be transformed to Nusselt numbers by making use of the well-established analogy between heat and mass transfer. From the standpoint of the experiments, the naphthalene technique offers important advantages compared to direct heat transfer measurements, including higher accuracy and significant apparatus simplifications.

During the execution of the experiments, mass transfer occurred at only one of the finned tubes of the array. That is, the exposed surfaces of only one of the finned tubes were of naphthalene, whereas the surfaces of the other finned tubes were of metal. In heat transfer terms, this is analogous to heat being transferred at one of the finned tubes, with the other tubes of the array being adiabatic. The practice of using a single active tube is a widely employed approach in research studies of tube banks.

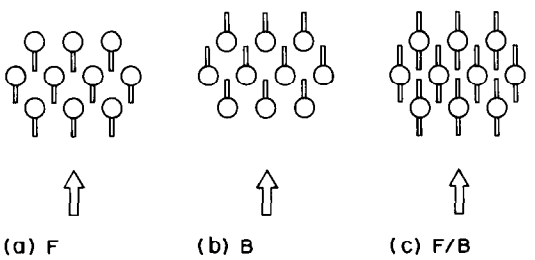

FIG. 4. Clusters of finned tubes illustrating the F, B and F/B configurations.

The mass transfer measurements were made at the centrally positioned tube in the seventh row. Prior experiments [1] had demonstrated that hydrodynamically developed conditions are established well upstream of that row.

The tube and the fin(s) which comprised the mass transfer active finned tube were separately coated with naphthalene and subsequently mated. The mating was accomplished by a tongue-in-groove arrangement. For this purpose, slots were milled into the tube, one at the upper end and one at the lower end. Correspondingly, each fin was fabricated with a pair of tongue-like extensions, positioned so as to mate with the aforementioned slots. Precise machining of the slots and the tongue-like extensions ensured that the mated fin emanated radially outward from the circumference of the tube and that the long dimension of the fin was parallel to the axis of the tube. The just-described method of fin-to-tube attachment was also used for the non-mass transfer tubes of the array (except at the side wall-adjacent half tubes, where the fins were attached to the side wall with double-stick tape).

The coating of a tube with naphthalene was accomplished by a multistep process. First, any residual naphthalene remaining from the preceding data run is removed by melting and evaporation. Then, Teflon inserts are placed in the slots at the ends of the tube. Next, using a continuous motion, the tube is dipped six or seven times in and out of a bath of molten naphthalene, with the first dipping performed sufficiently slowly as to form a clear coating well-bonded to the metal substrate. The final step in the process is a machining of the cylindrical surface of the fin on a lathe to yield the desired final dimensions and surface finish.

The coating of a fin is accomplished by a multiple-dipping process. By experimenting with the speed of the dipping motion and the temperatures of the molten naphthalene and the metal substrate, thin (~ 0.15 mm) reproducible coatings of good surface quality were obtained.

The determination of the mass transfer rate was based on the measurement of the change of mass of the naphthalene-coated finned tube which occurred between the beginning and the end of a data run. To accomplish these measurements, rapid access to the interior of the tube bank was necessary. To this end, the upper wall of the host duct was made removable, and quick-acting clamps, capable of being engaged or disengaged in seconds, were used to secure the wall in place.

The apparatus was operated in the suction mode, with air drawn from the laboratory into and through

the tube bank. The air exited the bank into a continuation of the host duct, from which it passed, via a square-to-circular transition section, to a flowmeter (a calibrated rotameter), a control valve, and a blower. The blower was situated in a service corridor adjacent to the laboratory. Its compression-heated, naphthalene-laden discharge was vented outside the building.

Each mass transfer data run was preceded by an equilibration period during which the tube bank (and, in particular, the naphthalene-coated finned tube) attained temperature equality with the air flow. During this period, sublimation was suppressed by a Teflon sheath which jacketed the coated finned tube. The mass of the coated finned tube was measured immediately preceding and immediately after the data run proper. Following the conclusion of the run, a calibration procedure was executed to account for possible extraneous sublimation during the handling of the finned tube. This yielded a correction of about 1%.

The mass measurements were made using an ultraprecision electronic analytical balance with a resolution of 10^{-5} g. The temperature was measured with an ASTM-certified thermometer with a smallest scale division of 0.1°F.

Pressure distribution

The streamwise pressure distribution along the tube bank was measured by means of a line of pressure taps installed in the upper wall of the host duct (the taps were centered between the side walls). To avoid their being covered by the fins, the taps were positioned so as to lie midway between the tips of adjacent, aligned B and F fins. There were seven such taps in the tube bank proper and five taps in the duct downstream of the bank.

The pressure distributions were measured in a set of data runs separate from the mass transfer runs. The pressure signals were detected by a capacitance-type pressure meter capable of resolving 10^{-3} Torr.

MASS/HEAT TRANSFER AND PRESSURE DROP RESULTS

Data reduction

As noted in the Introduction, two sets of mass/heat transfer results were evaluated, depending on the surface area used in the definition of the transfer coefficient. For one set, the coefficient is based on the actual transfer surface area A of the finned tube, while for the other set, the surface area A' ($= \pi DS$) of the unfinned tube is used.

If ΔM denotes the mass loss of the finned tube during a data run of duration τ, the mass transfer coefficients K and K' may be defined as

$$K = \frac{\Delta M/\tau A}{\rho_{nw} - \rho_{nb}}, \quad K' = \frac{\Delta M/\tau A'}{\rho_{nw} - \rho_{nb}}. \tag{3}$$

The quantities ρ_{nw} and ρ_{nb} respectively denote the naphthalene vapor densities at the finned tube surface and in the flow approaching the finned tube. The latter is zero for the present experiments, while the former was evaluated from the vapor pressure/temperature relation for naphthalene in conjunction with the perfect gas law.

The transfer coefficients K and K' can be expressed in dimensionless form via the Sherwood numbers

$$Sh = KD/\boldsymbol{D}, \quad Sh' = K'D/\boldsymbol{D} \tag{4}$$

in which the diffusion coefficient $\boldsymbol{D}$ can be eliminated by using the Schmidt number $Sc = \nu/\boldsymbol{D}$, where $Sc = 2.5$ for naphthalene diffusion in air.

The Sherwood number results will be parameterized by the Reynolds number

$$Re = V^*D/\nu. \tag{5}$$

The quantity V^* is a reference velocity in whose definition there is considerable flexibility. If $\dot{w}$ represents the air flow rate per lane of the tube bank (there are six lanes in the present tube bank as seen in Fig. 2(a)), V^* will be defined here as

$$V^* = \dot{w}/\rho(S_T - D)S. \tag{6}$$

Since the area $(S_T - D)S$ was fixed throughout the course of the experiments, V^* is a direct reflection of the air flow rate, as is the Reynolds number (since D was also fixed). Therefore, comparisons of results made at a fixed Reynolds number are equivalent to comparisons at a fixed mass flow rate. Note also that $(S_T - D)S$ is the minimum free-flow area per lane for an unfinned tube bank but is not the minimum free-flow area for a finned tube bank, as can be seen in Fig. 4.

The per-row fully developed pressure drop Δp for a tube bank is commonly expressed in dimensionless form via the ratio

$$f = \Delta p/\tfrac{1}{2}\rho V^{*2} \tag{7}$$

where f is often referred to as a friction factor. Note that for a fixed mass flow rate (i.e. fixed V^* and Re), any fin configuration-related changes in f are direct reflections of changes in Δp.

Two complementary approaches were employed to determine Δp. In one, the measured streamwise pressure distribution was fitted with a least-squares straight line, from which the pressure drop corresponding to a streamwise length S_L was evaluated. The second approach made use of the overall pressure drop measured between the ambient (from which the air was drawn) and the unobstructed duct downstream of the tube bank. Entrance and exit pressure losses were then subtracted, and the result was prorated among the rows, yielding Δp. In the majority of cases, the Δp values determined from the two approaches agreed to within 2%. The values of the entrance and exit losses needed in the second approach were determined from separate experiments conducted with an unfinned tube bank. It was assumed that these values would also be applicable to finned tube banks.

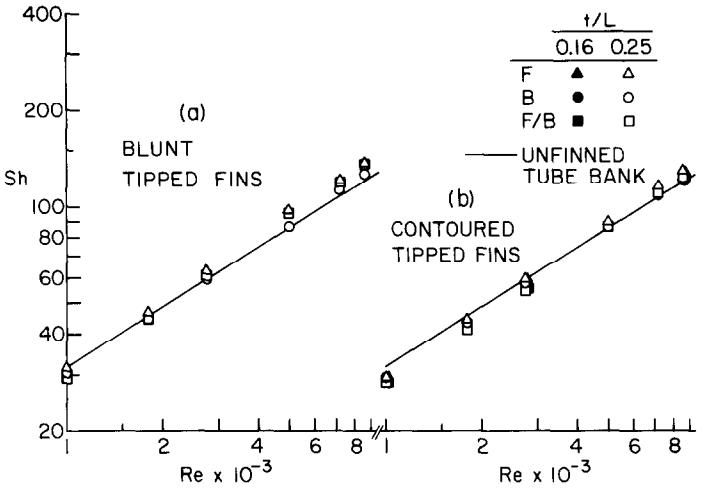

FIG. 5. Per-tube Sherwood numbers based on the actual transfer surface area.

Mass/heat transfer analogy

For heat transfer in cross-flow tube banks, all of the well-established correlations indicate that $Nu \sim Pr^n$. Therefore, in accordance with the analogy between mass and heat transfer, it follows that $Sh \sim Sc^n$ and that

$$Nu/Sh = (Pr/Sc)^n. \tag{8}$$

The present experiments provide Sherwood numbers corresponding to a Schmidt number of 2.5. With the aid of equation (8), these results can be transformed to Nusselt numbers corresponding to a given Prandtl number Pr. If $n = 0.36$ in accordance with the Zukauskas correlation [2], then

$$Nu = 0.719 Pr^{0.36} Sh_{2.5}. \tag{9}$$

In particular, for heat transfer in air ($Pr \simeq 0.7$),

$$Nu_{0.7} = 0.632 Sh_{2.5}. \tag{10}$$

In light of equation (9) (or equation (10)), the phrases mass transfer and heat transfer will be used interchangeably in the forthcoming presentation and discussion of results.

Sherwood/Nusselt number results

The per-tube Sherwood numbers for the hydrodynamically developed regime are presented in Figs 5 and 6. These Sherwood numbers pertain to a Schmidt number $Sc = 2.5$ but, in light of equations (9) or (10), they can, aside from a scale factor, be regarded as Nusselt numbers for any specified Prandtl number.

In Fig. 5, the mass transfer coefficient embedded in the Sherwood number is based on the actual transfer surface area of the finned tube. The figure is subdivided into parts (a) and (b) where, respectively, results are presented for tubes with blunt-tipped fins and with contoured-tipped fins. In each part of the figure, the Sherwood number is plotted as a function of the Reynolds number over the range from 1000 to about 9000. Different data symbols are used to identify the three fin configurations F (front), B (back), and F/B (front and back) that were illustrated in Fig. 4. For the blunt tipped case, the results correspond to a fin thickness $t/L = 0.25$, while the results for the contoured tipped case include both the $t/L = 0.16$ and 0.25 thicknesses.

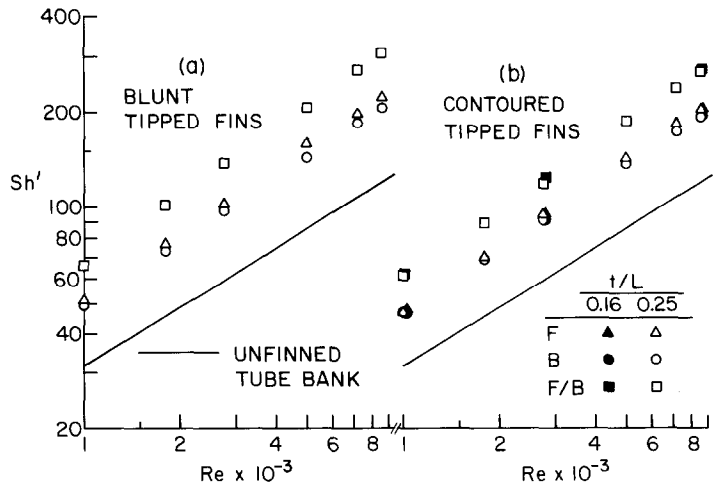

FIG. 6. Per-tube Sherwood numbers based on the surface area of an unfinned tube.

Sherwood number results for the same tube bank, but without fins, are depicted by the solid line which is drawn in each part of the figure. These results are taken from [1], and they are also in very good agreement with the Zukauskas correlation [2]. The unfinned tube Sherwood numbers serve as a baseline against which to compare the finned tube Sherwood numbers. Further, since the solid line is common to the two parts of the figure, it facilitates comparison of the Sherwood numbers for the blunt tipped and contoured tipped cases.

To assist in interpreting the results, it may be noted that a comparison of the Sherwood numbers for the various configurations at a fixed Reynolds number actually compares the mass/heat transfer rates per unit surface area at a fixed flow rate. An overall inspection of Fig. 5 indicates that the unit area mass transfer rate is not very sensitive to the presence or absence of the fins or to the specifics of the fin configuration. Indeed, the greatest deviation of the finned tube Sherwood numbers from those for the unfinned tube is about 15%. Therefore, the relative rates of mass transfer for the various configurations are more or less in proportion to their transfer surface areas, as will soon be documented.

The Reynolds number dependence of the finned tube results is slightly steeper than that of the unfinned tube results. At the low end of the Reynolds number range, the finned tube Sherwood numbers lie below those for the unfinned tube, while the opposite is true at the high end of the range. Among the finned configurations, the highest Sherwood numbers are attained by the front finned tube bank.

By comparing the (a) and (b) parts of the figure, it is evident that the unit area mass transfer rate is larger in the presence of blunt fins than with contoured tipped fins. The mass transfer enhancement associated with the bluntness is, however, modest—in the 5–10% range.

A comparison of the open and black symbols in Fig. 5(b) indicates that the unit area mass transfer is unaffected by the fin thickness in the investigated range. This insensitivity to thickness adds generality to the results. The $t/L = 0.25$ fin thickness was the largest that was thought to be of practical interest, while the $t/L = 0.16$ thickness was about the smallest that could be conveniently used in the present experimental setup.

An alternative presentation of the per-tube mass transfer results is conveyed by Fig. 6. Here, the mass transfer coefficient embedded in the Sherwood number Sh' is based on the surface area A' of the unfinned tube. Since A' is common to all of the cases dealt with in Fig. 6, Sh' serves as a dimensionless representation of the mass transfer rate. Thus, comparisons of the Sh' values for the various configurations at a given Reynolds number are equivalent to a comparison of mass transfer rates at a given flow rate. Aside from the change of the ordinate variable from Sh to Sh', the format of Fig. 6 is the same as that of Fig. 5.

A comparison of the finned tube and unfinned tube data in Fig. 6 reveals the enhancement of the mass transfer rate due to finning. These enhancements are appreciable and reflect the ratio of the transfer surface areas of the finned and unfinned tubes. The F/B configuration, whose surface area is about 2.2 times that of the unfinned tube, yields mass transfer enhancements of comparable extent. The area ratios for the F and B configurations are equal to about 1.6, and the mass transfer enhancements are in this same range, with that for the F configuration being somewhat greater.

Table 1. Ratios of the finned-tube surface area to the unfinned-tube surface area

Case	Blunt	Contoured $t/L = 0.16$	Contoured $t/L = 0.25$
F or B	1.637	1.610	1.586
F/B	2.273	2.219	2.173

A quantitative comparison of the mass transfer enhancement ratio and the surface area ratio is facilitated by examination of Tables 1 and 2. The area ratios are listed in Table 1, while Table 2 lists the ratios of the mass transfer rates for finned and unfinned tubes at the smallest and largest Reynolds numbers in the investigated range. The blunt tipped fin results of Table 2 are for $t/L = 0.25$, while the contoured tipped fin results apply equally well for $t/L = 0.16$ and 0.25.

Tables 1 and 2 show that the mass transfer enhancement ratio is greater than the corresponding area ratio at the high Reynolds numbers but falls below the area ratio at the low Reynolds numbers. Table 2 confirms that the F configuration yields higher mass transfer rates than does the B configuration, as do the blunt tipped fins compared with the contoured tipped fins.

The Sherwood number results that have been presented in this section of the paper will be employed in a performance analysis that will follow shortly.

Pressure drop results

The dimensionless per-row pressure drop f is plotted in Fig. 7 as a function of the Reynolds number for the various fin configurations (F, B and F/B), tip types, and thicknesses. Also plotted for reference purposes is a dashed line depicting the f results for the unfinned tube bank. These results, obtained here as a prelude to the finned tube experiments, are in very good agreement with those of Zukauskas [2].

Turning first to the results for tubes with blunt tipped fins, it is seen that relatively high pressure drops (about

Table 2. Ratios of mass transfer rates for finned and unfinned tubes

Case	Blunt $Re = 1000$	Blunt $Re = 8600$	Contoured $Re = 1000$	Contoured $Re = 8600$
F	1.612	1.859	1.470	1.700
B	1.555	1.724	1.470	1.606
F/B	2.084	2.565	1.931	2.233

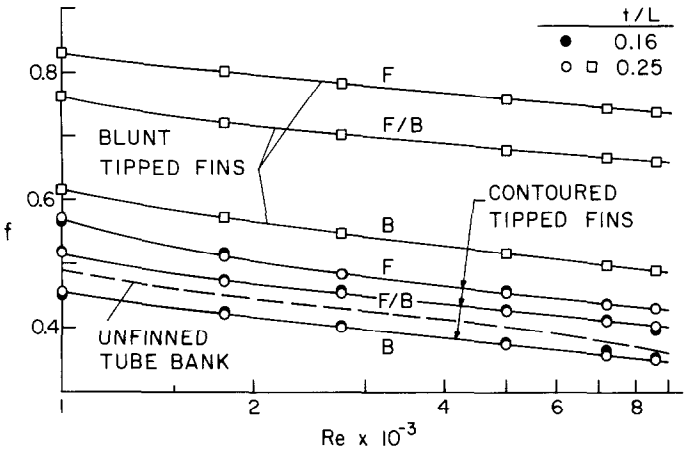

FIG. 7. Dimensionless per-row pressure drops.

80% greater than those for the unfinned tube bank) are sustained for configuration F (front fins). On the other hand, the pressure drops for configuration B (back fins) are only about one-third greater than the unfinned-tube values. The substantially higher pressure drop for the F configuration is due to the losses associated with the flow separation at the blunt forward-facing fin tip. It is noteworthy that the pressure drop for the F/B configuration lies below that for the F configuration. This lesser pressure drop may be attributed to a decrease in the aforementioned losses at the blunt, forward-facing tip. The decrease occurs because of the flow channeling which is inherent in the F/B configuration, as suggested by reference to Fig. 4(c). The channel flow does not impact squarely on the forward-facing tip.

The pressure drops for the contoured finned tubes are substantially lower than those for the blunt finned tubes and, in addition, the spread among the results for the F, B and F/B configurations is much smaller, although the ordering remains as before. Even for the F configuration, the pressure drop is only about 15% greater than that for the unfinned tube bank. Of even greater note, however, is that the B-configuration pressure drops are lower (by about 7%) than the unfinned tube values.

The foregoing discussion was focused on the results for the $t/L = 0.25$ thickness fins (the open data symbols). Figure 7 also conveys pressure drop results for the thinner ($t/L = 0.16$) contoured fins, which are represented by black symbols. It can be seen that the two sets of results are in very good agreement, with deviations confined to the 2% range. This insensitivity of the pressure drop to the fin thickness reinforces a similar finding from the mass transfer results (Figs 5 and 6).

PERFORMANCE EVALUATION

In preceding sections of the paper, it was demonstrated that the use of fins to add surface area can bring about substantial increases in the tube-bank heat transfer. The presence of the fins also affects the pressure drop characteristics of the tube bank. It still remains to assess the relative merits of the configurations F, B and F/B and of the blunt and contoured tip treatments (the results were shown to be insensitive to the fin thickness in the investigated range). Such an assessment will be made by comparing the heat transfer rates for the various finned tube banks (and the unfinned tube bank) under each of the following constraints: (a) fixed pumping power, (b) fixed pressure drop, and (c) fixed mass flow.

It is also relevant to compare the heat transfer enhancements due to finning with those obtainable by employing other means of increasing the surface area. One easily implemented means of increasing the area is to increase the tube diameter (without finning). The enhancements due to finning and to increased tube diameter will be compared at equal transfer surface area in the performance assessment which follows. The equal-area heat transfer rates for the two classes of tube banks are compared at fixed pumping power, fixed pressure drop, and fixed mass flow.

All of the tube banks to be considered in the performance assessment are equilateral triangular arrays, with the tube centers being common to all of the banks (common values of S_T and S_L). In addition, the tube length S and the number of tubes per row are also in common. Furthermore, the comparisons will be focused on the hydrodynamically developed regime.

The methodology of the performance assessment will now be outlined. To begin, a baseline case is selected that will serve as a standard against which the results for all cases (i.e. both finned tube banks and unfinned tube banks) will be compared. The baseline is the *unfinned*, equilateral triangular array with $S_T/D = 2$. This case is selected because it is the actual base case to which fins were added during the present investigation. As noted earlier, the heat (mass) transfer and pressure drop results for the base case, as determined using the present apparatus, are virtually identical to those of the literature [2]. The base case will be identified by the subscript o, and the corresponding per-tube heat

transfer rate (for a specified Reynolds number Re_o) and surface area are Q_o and A_o.

Suppose that the per-tube heat transfer rate Q for some other case (i.e. a finned or an unfinned tube bank) is to be compared with that for the base case for a fixed value of a parameter χ (either pumping power or pressure drop or mass flow). Rather than select χ directly, it was found convenient to pick a value of Re_o and then evaluate the corresponding χ for the baseline case; Q_o and other quantities of interest for the baseline case are also evaluated for the selected Re_o. Then, turning to the other case which is to be compared with the base case and using the aforementioned value of χ as input, the Reynolds number Re is determined (in general, $Re \neq Re_o$). For this Re value, Q and other quantities of interest are computed for the other case. Then, Q/Q_o and other relevant ratios (relative to the base case) are evaluated.

In actuality, several cases (i.e. various finned and unfinned tube banks) are to be compared to the base case for the fixed value of χ corresponding to the selected Re_o, yielding a set of Q/Q_o ratios. Since Q_o is common to all, the relative magnitudes of the Q/Q_o ratios enable the various cases to be rank ordered according to Q.

In computing the performance ratios for the different-diameter unfinned tube banks, the Nusselt number and pressure drop results of Zukauskas [2] were employed. The latter are available for $S_T/D = 1.25$, 1.5, 2 and 2.5.

If the analogy between mass and heat transfer, as expressed by equation (9), is employed to transform the Sherwood numbers to Nusselt numbers, the performance comparisons are independent of the Prandtl and Schmidt numbers.

Fixed pumping power

The pumping power PP per lane and per row of a tube bank may be expressed as

$$PP = (\dot{w}/\rho)\Delta p \tag{11}$$

where $\dot{w}$ is the mass flow rate per lane and Δp is the pressure drop per row. Equation (11) may be rephrased by eliminating Δp in favor of f via equation (7), $\dot{w}$ in favor of V^* via equation (6), and V^* in favor of Re via equation (5), with the result

$$PP/\psi = fRe^3\alpha^2(\alpha-1) \tag{12}$$

where

$$\psi = \tfrac{1}{2}(\mu^3/\rho^2)(S/S_T^2), \quad \alpha = S_T/D. \tag{13}$$

Note that both the tube length S and the transverse pitch S_T are constant for all of the investigated arrays, so that for constant properties, ψ is also a constant. Therefore, PP/ψ can be regarded as the constrained parameter χ for the fixed pumping power comparison, i.e.

$$\chi_{pp} = fRe^3\alpha^2(\alpha-1). \tag{14}$$

If χ_{pp} is evaluated for the base case, then $Re = Re_o$, $f = f_o(Re_o)$, and $\alpha = \alpha_o = 2$, so that

$$\chi_{pp} = 4f_oRe_o^3. \tag{15}$$

For all the finned tube banks investigated here, $\alpha = 2$. If equation (14) is applied to any one of the finned tube banks and χ_{pp} is eliminated via equation (15), there follows

$$fRe^3 = f_oRe_o^3. \tag{16}$$

For each finned tube bank, equation (16) can be solved for the value of Re corresponding to the given Re_o.

For the different-diameter unfinned tube banks, α varies from case to case. The application of equation (14) to such a tube bank yields, after elimination of χ_{pp},

$$fRe^3 = f_oRe_o^3[4/\alpha^2(\alpha-1)] \tag{17}$$

which can be solved for Re.

With Re_o for the base case and with the Re values for the finned tube and unfinned tube comparison cases, the corresponding Nusselt numbers can be evaluated (Fig. 6 for the finned tube cases and equation (40) of [2] for the unfinned tube cases). The Q/Q_o ratios deduced from these Nusselt numbers are plotted in Fig. 8 as a function of the surface area ratio A/A_o. Results are presented for three different levels of pumping power, respectively identified by the indicated values of Re_o. To separate the results for the three Re_o, shifted ordinate scales have been used.

The results for the finned tube banks are shown as discrete symbols identified in Fig. 8, while those for the different-diameter unfinned tube banks are represented by continuous curves. Note that the latter terminate at $A/A_o = 1.6$, which corresponds to $S_T/D = 1.25$ (the smallest S_T/D for which f values are available in [2]). For the limiting unfinned tube bank characterized by $S_T/D = 1$ (tube-to-tube contact), $A/A_o = 2$.

For all cases, $Q/Q_o > 1$ when $A/A_o > 1$, so that the

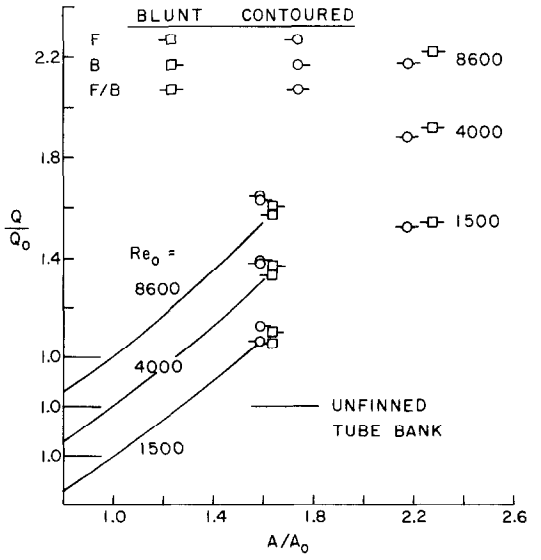

FIG. 8. Comparisons of heat transfer rates at fixed pumping power.

addition of area is enhancing. The enhancement (i.e. the magnitude of Q/Q_o) is greater at higher Re_o.

As seen in Fig. 8, the only area ratio common to the investigated finned and unfinned tube banks is $A/A_o \simeq 1.6$ (F and B fin configurations). At that area ratio, the two methods of adding surface area (i.e. finning and increased tube diameter) yield generally similar heat transfer enhancements on a fixed pumping power basis. Finning affords a modest advantage in Q/Q_o when contoured fins are used and at larger Reynolds numbers.

The F/B configuration yields heat transfer enhancements substantially greater than those attainable with increased-diameter unfinned tubes. This is because finning enables the use of larger surface areas than are possible with unfinned tubes.

With regard to comparisons among the various finned tube banks, it is seen that contouring is moderately advantageous, with the greatest benefit occurring for F fins at larger Reynolds numbers. As concerns the issue of B vs F positioning, the B position is advantageous for blunt tipped fins, but not consistently so for contoured tipped fins.

It is also of interest to examine the flow rate and pressure drop relationships which correspond to the fixed pumping power constraint. Note that at a fixed value of the pumping power, $\dot{w}/\dot{w}_o = \Delta p_o/\Delta p$. The $\dot{w}/\dot{w}_o$ ratio for a finned tube bank is easily shown to be

$$\dot{w}/\dot{w}_o = Re/Re_o \tag{18}$$

while for different-diameter unfinned tube banks

$$\dot{w}/\dot{w}_o = [Re(\alpha-1)]/[Re(\alpha-1)]_o \tag{19}$$

where $\alpha_o = 2$.

The $\dot{w}/\dot{w}_o$ ($= \Delta p_o/\Delta p$) ratios are plotted in Fig. 9 as a function of A/A_o for parametric values of Re_o (i.e. parametric values of pumping power). The results corresponding to $Re_o = 1500$ and 8600 fall in close proximity to each other, necessitating the omission of the $Re_o = 4000$ case to preserve clarity. It is seen from Fig. 9 that, relative to the base case, both finning and increases in tube diameter at fixed pumping power give rise to lower flow rates and higher pressure drops. However, the departures from the base case are much more moderate in the presence of finning than for increased-diameter unfinned tubes. As a result, at a given area ratio (e.g. $A/A_o \simeq 1.6$), the mass flow through a finned tube bank is substantially greater than that through an increased-diameter unfinned tube bank, while the pressure drop is significantly lower.

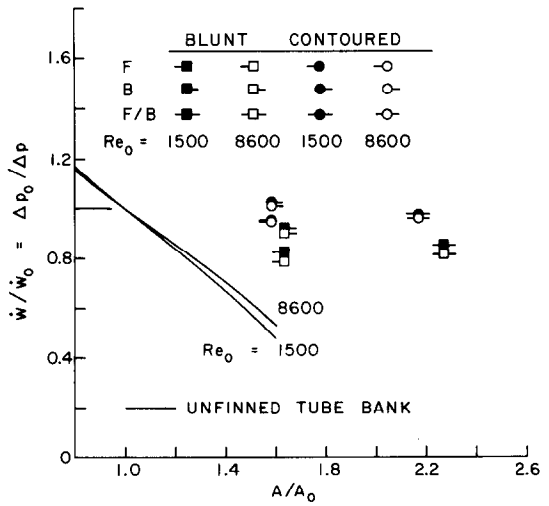

FIG. 9. Mass flow and pressure drop relationships at fixed pumping power.

Thus, whereas the equal-area ($A/A_o \simeq 1.6$) Q/Q_o ratios for the two classes of tube banks are not very different (Fig. 8), the $\dot{w}/\dot{w}_o$ ($= \Delta p_o/\Delta p$) ratios are decidedly different. In view of this, mass flow and pressure drop considerations may be the pivotal factors in the choice of finning vs an increase in diameter.

Note that for the tube bank with contoured B fins, $\dot{w}$ actually exceeds $\dot{w}_o$. This is because the friction factors for this case are lower than those for the base case at all Reynolds numbers (Fig. 7).

Fixed pressure drop

The Re, Re_o relationships for fixed per-row pressure drop ($\Delta p = \Delta p_o$) are derived in a manner similar to that for the fixed pumping power constraint. Corresponding to equations (16) and (17), there are now obtained

$$fRe^2 = f_o Re_o^2 \tag{20}$$

$$fRe^2 = f_o Re_o^2 (4/\alpha^2) \tag{21}$$

where $\alpha_o = 2$ has been used. A given value of Re_o is now equivalent to a fixed value of the per-row pressure drop. Equations (20) and (21) are employed to solve for the Re values corresponding to the given Re_o and, with these, the relevant Nusselt numbers are determined to yield the Q/Q_o ratios.

The Q/Q_o ratios corresponding to the fixed pressure drop constraint are plotted in Fig. 10 as a function of the surface area ratio A/A_o. Results are given for two different levels of pressure drop respectively characterized by $Re_o = 1500$ and 8600. The discrete data correspond to the finned tube banks (the symbol definition is identical to that of Fig. 9), while the continuous curves are for the different-diameter unfinned tube banks.

Examination of Fig. 10 shows that for fixed pressure drop, finning yields substantially greater heat transfer enhancement than does the use of increased-diameter unfinned tubes. For example, for $Re_o = 8600$ and $A/A_o \simeq 1.6$, $Q/Q_o = 1.62$ for the contoured-finned tube banks (either F or B), while $Q/Q_o = 1.23$ for the increased-diameter unfinned tube bank. The two-fold enhancement afforded by the F/B finned tube bank is well out of reach of the unfinned tube banks.

Contouring of the fin tips appears to be advantageous for all configurations. Also, the B configuration generally yields higher Q values than does the F configuration. For both the finned and the

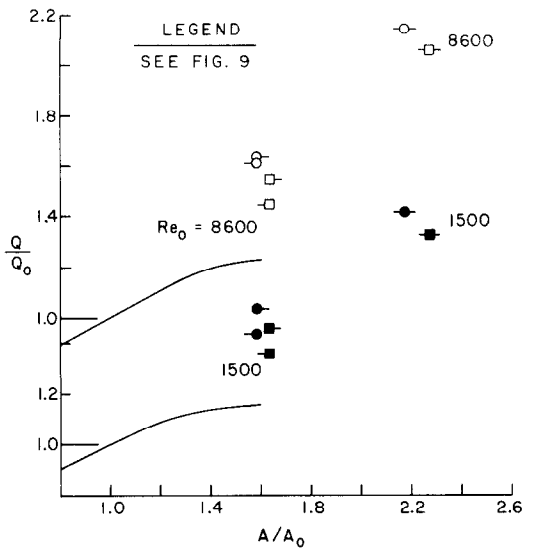

FIG. 10. Comparisons of heat transfer rates at fixed pressure drop.

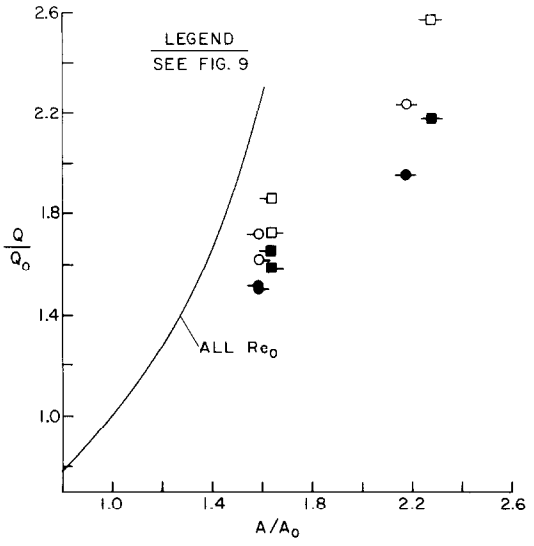

FIG. 12. Comparisons of heat transfer rates at fixed mass flow.

increased-diameter unfinned tube banks, greater enhancement (i.e. larger Q/Q_0) is in evidence at higher Re_0 (higher levels of pressure drop).

The mass flow and pumping power relationships corresponding to the fixed pressure drop constraint will now be examined. With $\Delta p = \Delta p_0$, it follows that

$$\dot{w}/\dot{w}_0 = PP/PP_0. \tag{22}$$

Equations (18) and (19) for $\dot{w}/\dot{w}_0$ continue to be valid, with input values of Re and Re_0 appropriate to the fixed pressure drop constraint.

The $\dot{w}/\dot{w}_0 (= PP/PP_0)$ ratios are plotted as a function of A/A_0 in Fig. 11. As seen there, the enhanced tube banks (i.e. those with $A/A_0 > 1$) are generally characterized by lower mass flows and lower pumping power requirements than the base case. At a given surface area (i.e. given A/A_0), both $\dot{w}$ and PP are higher for finned tube banks than for increased-diameter, unfinned tube banks.

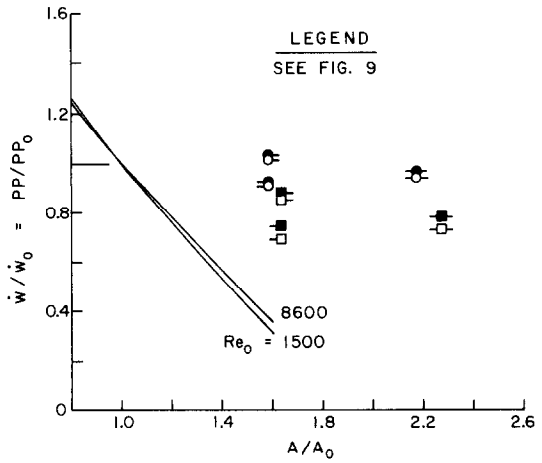

FIG. 11. Mass flow and pumping power relationships at fixed pressure drop.

Fixed mass flow

The translation of the fixed mass flow constraint into a relationship between Re_0 and Re is accomplished by using equations (5) and (6). For the finned tube banks, there is obtained

$$Re = Re_0 \tag{23}$$

while for the different-diameter unfinned tube banks

$$Re = Re_0/(\alpha - 1). \tag{24}$$

In these equations, a given value of Re_0 is equivalent to a fixed value of the mass flow. With these Re_0 and Re, Nusselt numbers and Q/Q_0 ratios are determined.

The fixed mass flow Q/Q_0 ratios plotted in Fig. 12 display characteristics that differ from those for the preceding constraints. For one thing, the finned tube Q/Q_0 ratios are well below those for the increased-diameter unfinned tubes. At the common area ratio $A/A_0 \simeq 1.6$, the Q/Q_0 range for the various finned tube banks is from 1.5 to 1.85, while the Q/Q_0 ratio for the increased-diameter unfinned tube banks is 2.3. Also, for fixed $\dot{w}$, the blunt fins have higher Q/Q_0 values than the contoured fins, and similarly for the F configuration relative to the B configuration. As will be documented shortly, these characteristics are related to the fact that the fixed mass flow constraint is unmindful of pressure drop and pumping power ramifications.

By employing equations (5) and (7), the $\Delta p/\Delta p_0$ ratio can be expressed as

$$\Delta p/\Delta p_0 = [\alpha^2 f Re^2]/[\alpha^2 f Re^2]_0 \tag{25}$$

with $\alpha_0 = 2$. Also, for fixed mass flow, $\Delta p/\Delta p_0 = PP/PP_0$.

Equation (25) has been evaluated for the Re_0 and Re values relevant to the fixed mass flow constraint, and the results are plotted in Fig. 13. The figure shows that the pressure drop and pumping power for the increased-diameter unfinned tube banks are very much

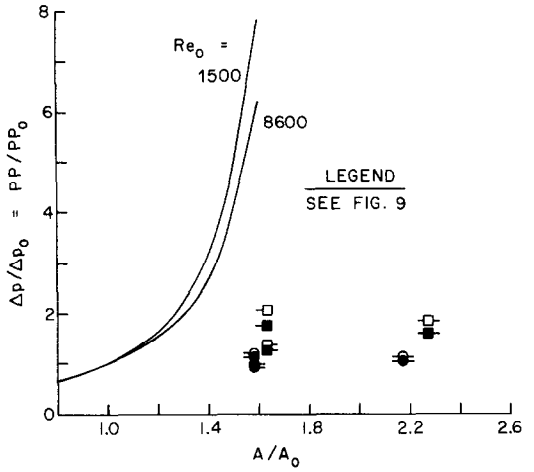

FIG. 13. Pressure drop and pumping power relationships at fixed mass flow.

higher than those for the finned tube banks. At $A/A_o \simeq 1.6$, the former lie in the range $\Delta p/\Delta p_o = 6.2$–$7.8$, while the latter range from 0.94 to 2.05. The high pressure drop penalty that is paid by the unfinned tube bank for greater heat transfer enhancement is, thus, readily apparent. Also, the pressure drop for the blunt fins is greater than that for the contoured fins, and similarly for the *F* configuration relative to the *B* configuration.

CONCLUDING REMARKS

The heat transfer and pressure drop response of a cross-flow tube bank to the presence of longitudinal fins attached to the individual tubes of the array has been determined experimentally. The investigated tube banks are intended to model either a cross-flow heat exchanger or an array of pin fins.

Several fin configurations were employed during the course of the experiments. In one, the fins were attached only at the fronts of the tubes, while in another the fins were attached only at the rear. In a third configuration, fins were attached at both the front and rear. The effect of the shape of the fin tip was also investigated and, in this regard, both blunt tipped and contoured tipped fins were employed. The fin thickness was also varied.

For each tube bank geometry, the per-tube heat transfer coefficient and the per-row pressure drop were measured in the hydrodynamically developed regime over a nine-fold variation of the Reynolds number. These results showed that a high degree of heat transfer enhancement can be achieved by finning and also indicated the associated pressure drop penalty (in certain cases, finning actually reduced the pressure drop relative to the corresponding unfinned tube). The performance of the various tube banks was compared at fixed pumping power, fixed pressure drop, and fixed mass flow.

The heat transfer enhancements obtained by finning were compared with those attainable by the use of increased-diameter unfinned tubes. For the same pressure drop, finning yields significantly greater enhancements. At fixed mass flow, greater enhancements are attained with increased-diameter unfinned tubes, but at a high penalty in pressure drop and pumping power. For the same pumping power, the two methods of adding surface area yield comparable enhancements, with that for finning being slightly greater. It is also noteworthy that for an array with fixed tube centers, greater additions of surface area are possible by finning than by increases in tube diameter.

REFERENCES

1. E. M. Sparrow and R. Ruiz, Effect of blockage-induced flow maldistribution on the heat transfer and pressure drop in a tube bank, *J. Heat Transfer* **104**, 691–699 (1982).
2. A. A. Zukauskas, Heat transfer from tubes in crossflow. In *Advances in Heat Transfer*, Vol. 8, pp. 93–160. Academic Press, New York (1972).

ARRANGEMENTS DE TUBES AILETES LONGITUDINALEMENT EN ATTAQUE FRONTALE ET LEURS CARACTERISTIQUES DE TRANSFERT THERMIQUE ET DE PERTE DE CHARGE

Résumé—Des expérimentations de transfert thermique et de perte de charge sont conduites sur des arrangements de tubes en courants croisés dans lesquels les tubes sont équipés d'ailettes longitudinales. Les paramètres géométriques étudiés incluent le positionnement des ailettes (devant le tube, à l'arrière, et à la fois devant et derrière), la forme du sommet et l'épaisseur de l'ailette. Pour chaque géométrie de l'arrangement, le nombre de Reynolds varie approximativement d'un ordre de grandeur. Les résultats montrent qu'un fort accroissement du transfert thermique peut être obtenu par l'ailetage, et les accroissements pour différentes géométries du faisceau de tubes sont comparés pour une même puissance de pompage, pour une perte de charge fixée ou pour un débit-masse fixé. Les accroissement sont aussi comparés à ceux obtenus par un accroissement du diamètre des tubes lisses. L'ailetage est spécialement avantageux quand la comparaison est faite à une perte de charge fixée. Pour un arrangement avec les centres des tubes fixés, les ailettes permettent des plus forts accroissements de surface que par des augmentations du diamètre du tube.

LÄNGSBERIPPTE, QUER ANGESTRÖMTE ROHRBÜNDEL UND IHRE WÄRMEÜBERGANGS-UND DRUCKABFALL-EIGENSCHAFTEN

Zusammenfassung—Es wurden Wärmeübergangs- und Druckabfallsmessungen an quer angeströmten Rohrbündeln durchgeführt, wobei die einzelnen Rohre mit Längsrippen versehen waren. Die untersuchten geometrischen Parameter waren u.a. die Anordnung der Rippen (auf der Vorderseite des Rohres, auf der Rückseite und auf Vorder- und Rückseite), die Form der Rippenspitze (stumpf oder geformt) und die Rippendicke. Für jede Rohrbündelgeometrie wurde die Reynolds-Zahl um fast eine Größenordnung verändert. Die Ergebnisse zeigen, daß eine starke Verbesserung des Wärmeübergangs durch die Berippung erreicht wird. Die Verbesserung bei den verschiedenen Rohrbündelgeometrien wird bei konstanter Gebläseleistung, konstantem Druckabfall und konstantem Massenstrom verglichen. Die rippenbezogenen Verbesserungen werden auch mit denen verglichen, die sich beim Einsatz von unberippten Rohren mit vergrößertem Durchmesser erzielen lassen. Dabei ist die Berippung insbesondere dann vorteilhaft, wenn der Vergleich bei konstantem Druckabfall erfolgt. Liegen die Rohrachsen fest, so erlaubt die Berippung eine größere Oberflächenzunahme im Vergleich zu einer Vergrößerung des Rohrdurchmessers.

ТЕПЛОПЕРЕНОС И ПЕРЕПАД ДАВЛЕНИЯ В ПРОДОЛЬНО ОРЕБРЕННЫХ, ПОПЕРЕЧНО ОБТЕКАЕМЫХ ПУЧКАХ ТРУБ

Аннотация—Проведено экспериментальное исследование теплопереноса и перепада давления в поперечно обтекаемых пучках труб, в которых отдельные трубы имели продольное оребрение. Исследовались следующие геометрические параметры: местоположение ребер (в начале или в конце трубы, в ее начале и конце одновременно), форма верхней части ребра (скругленная или заостренная) и толщина ребра. Для каждой геометрии пучка труб значения числа Рейнольдса изменялись примерно на порядок. Результаты показывают, что за счет оребрения можно достичь очень высокой степени интенсификации процесса теплопереноса. Проведено сравнение роста интенсивности теплопереноса для различных геометрий пучков при фиксированных значениях расхода энергии на привод насоса, перепада давления и массового расхода. Рост переноса тепла за счет оребрения сравнивался также с результатами, полученными при использовании неоребренных труб большего диаметра. Показано, что результаты по эффективности оребрения оказываются наиболее хорошими, если сравнение проводится при фиксированном перепаде давления. В пучках с фиксированными центрами труб за счет оребрения можно получить большую площадь поверхности теплообмена, чем при увеличении диаметра труб.